Ab Initio Study of Phosphorescent Emitters Based on Rare-Earth Complexes with Organic Ligands for Organic Electroluminescent Devices

ARTICLE *in* THE JOURNAL OF PHYSICAL CHEMISTRY A · MAY 2011

Impact Factor: 2.69 · DOI: 10.1021/jp111303a · Source: PubMed

4 AUTHORS, INCLUDING:

Alexandra Freidzon
Russian Academy of Sciences
31 PUBLICATIONS **180** CITATIONS
SEE PROFILE

A. V. Scherbinin
Lomonosov Moscow State University
37 PUBLICATIONS **292** CITATIONS
SEE PROFILE

Alexander Bagaturyants
Russian Academy of Sciences
196 PUBLICATIONS **928** CITATIONS
SEE PROFILE

THE JOURNAL OF PHYSICAL CHEMISTRY A

ARTICLE

pubs.acs.org/JPCA

Ab Initio Study of Phosphorescent Emitters Based on Rare-Earth Complexes with Organic Ligands for Organic Electroluminescent Devices

Alexandra Ya. Freidzon,*[,†] Andrei V. Scherbinin,[‡] Alexander A. Bagaturyants,[†] and Michael V. Alfimov[†]

[†]Photochemistry Center, Russian Academy of Sciences, ul. Novatorov 7a, Moscow, 119421 Russia

[‡]Chemistry Department, Moscow State University, 119991 Moscow, Russia

Supporting Information

ABSTRACT: An ab initio approach is developed for calculation of low-lying excited states in Ln^{3+} complexes with organic ligands. The energies of the ground and excited states are calculated using the XMCQDPT2/CASSCF approximation; the 4f electrons of the Ln^{3+} ion are included in the core, and the effects of the core electrons are described by scalar quasirelativistic 4f-in-core pseudopotentials. The geometries of the complexes in the ground and triplet excited states are fully optimized at the CASSCF level, and the resulting excited states have been found to be localized on one of the ligands. The efficiency of ligand-to-lanthanide energy transfer is assessed based on the relative energies of the triplet excited states localized on the organic ligands with respect to the receiving and emitting levels of the Ln^{3+} ion. It is shown that ligand relaxation in the excited state should be properly taken into account in order to adequately describe energy transfer in the complexes. It is demonstrated that the efficiency of antenna ligands for lanthanide complexes used as phosphorescent emitters in organic light-emitting devices can be reasonably predicted using the procedure suggested in this work. Hence, the best antenna ligands can be selected in silico based on theoretical calculations of ligand-localized excited energy levels.

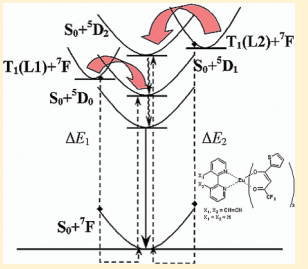

INTRODUCTION

The efficiency of organic light-emitting devices (OLEDs) depends on the utilization of both singlet and triplet excitons formed in the emitting layer (see, for example, refs 1−3). In fluorescent emitting materials, only singlet excitons can recombine to produce light. However, according to spin statistics, the ratio of triplet to singlet excitons generated in the material due to electron−hole recombination is 3:1. To efficiently utilize triplet excitons and attain up to 100% quantum efficiency of light emission, the emitting layer is doped with phosphorescent emitters, in particular, complexes of heavy and rare-earth metals with organic ligands.[4−7]

In lanthanide complexes, the central ion serves as an emitter and excitation energy is transferred to it through its ligands from the host material. The mechanism of energy transfer is rather complicated, and some relevant models will be described below.

The emission of Ln^{3+} complexes is due to f−f transitions of the central ion (Ln^{3+}). Such transitions are parity forbidden in the free ion. In organometallic complexes (embedded in an organic matrix in OLED systems), however, they become allowed because of symmetry violation in the ligand field and vibronic coupling effects, which can effectively relax the selection rules. In such systems, the emitting states of the central ion can be pumped through nonradiative excitation energy transfer from the organic host material to the ligands and then to the central ion.

The efficiency of energy transfer in the emitting layer of OLEDs is controlled by the relative positions of the excited levels in the emitting ion, in the ligands, and in the host material. Hence, the problem of attaining maximum performance of the emitting layer breaks up into two, namely, predicting the ligands that ensure most efficient energy transfer to a particular lanthanide and predicting the host materials that match the chosen ligands best. In this paper, we will focus on the first problem.

Quantum-chemical calculations provide important information about the excited ligand levels, which can be used to estimate the efficiency of energy transfer. Correlations between the ligand structure and its capacity to transfer excitation to the lanthanide ions can be drawn after an extensive computational study of potential emitters. Thus, screening of potential emitting complexes can be performed in silico, by computer simulation, without laborious and expensive synthesis of numerous compounds, whose emitting capacity is questionable.

It was observed in refs 8 and 9 that the lowest triplet energy of the ligand correlates with the luminescence quantum yield of Ln^{3+} complexes. The highest quantum yields are obtained when the lowest triplet state of the ligand matches certain excited levels of the Ln^{3+} ion. Further experimental and theoretical results supported the hypothesis that the ligand-localized triplet states play an essential role in energy transfer to Ln^{3+} (see next section).

A semiempirical sparkle model for calculations of lanthanide complexes (SMLC) was proposed in refs 1 and 2. It was successfully used for calculations of the equilibrium structures of Ln^{3+}

Received: November 28, 2010
Revised: March 26, 2011
Published: April 19, 2011

Scheme 1. Phosphorescent Eu^{3+} Complexes Studied in This Work

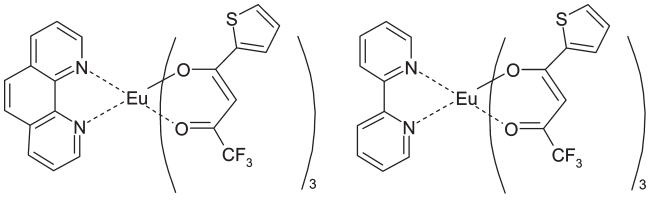

Eu(*tta*)$_3$*phen* Eu(*tta*)$_3$*bipy*

complexes in the ground state (combined with a semiempirical quantum-chemical method like AM1 or PM6, etc.) and their vertical excitation energies (combined with the INDO/S−CI technique).[10,11,3−27] In the SMLC, the Ln^{3+} ion was approximated by a point charge in the center of a repulsive spherical potential of the form $\exp(-\alpha r)$.

On the basis of the calculated energy levels, various energy-transfer mechanisms and corresponding kinetic models were proposed in these papers to calculate energy-transfer rates and emission quantum yields.[13−17,19−26,28] It was mentioned, however, that the accuracy of excitation energies obtained using the semiempirical methods was not sufficient, and therefore, the experimental rather than theoretical values were used in ref 26 to estimate the energy-transfer rate between the excited ligand state and the ligand-to-metal charge-transfer (LMCT) state.

In some works, the positions of ligand-localized triplet excited levels in Ln^{3+} complexes were calculated by DFT.[29−35] Scalar quasirelativistic 4f-in-core pseudopotentials[36,37] were used to describe the Ln^{3+} ion in these calculations, and TDDFT (a recent review see in ref 38) was mostly used in these works to calculate triplet excited states. An unrestricted DFT formalism without employing time-dependent theory was also used for this purpose in refs 33−35.

However, DFT-based methods, as discussed in ref 39, can underestimate the relative stability of high-spin states in molecules and produce excessively delocalized charge distributions, even with the Hartree−Fock exchange partially included (see ref 39 and references therein). This means that DFT cannot predict the correct localization of triplet excited states. It is also known well that TDDFT predicts erroneously low energies of charge-transfer excited states.[40]

In this work, we propose a systematic ab initio approach to predicting transition energies for low-lying ligand-localized excited states of Ln^{3+} complexes. The approach employs wave function-based methods adequate for quasi-degenerate states. It is based on a multireference CASSCF technique for the calculations of the ground and excited states of the Ln^{3+} complex, the corresponding equilibrium geometries of the complex, and the energies of excitations localized on organic ligands in the Ln^{3+} complex. Like in the majority of other calculations, relativistic effects and effects of 4f electrons are taken into account using the scalar quasirelativistic 4f-in-core pseudopotentials with the corresponding basis sets[36,37] for the Ln^{3+} ion. Note that the 4f-in-core pseudopotentials[36,37] were specifically derived to describe the Ln^{3+} ions with fixed f-shell occupations.

In this approach, the excited states of the complex corresponding to 4f−4f excitations cannot be considered directly. Because 4f orbitals of a lanthanide are strongly localized near the nucleus, they only slightly interact with the ligands. As a result, the emitting 4f−4f

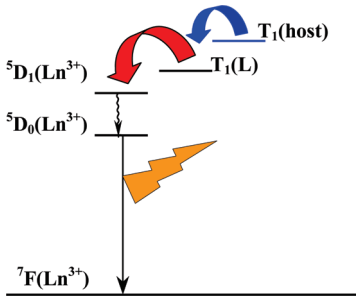

Figure 1. Stepwise excitation energy transfer from the host to the emitter in the emitting layer of OLED.

excited levels of Ln^{3+} are almost insensitive to the chemical environment of the ion. Therefore, the observed 4f−4f emission bands are rather narrow and nearly coincide for different compounds of a given lanthanide. Hence, it is reasonable to consider that the relative energies of the 4f−4f excited levels of Ln^{3+} in different complexes can simply be taken from the experimental data for the free ions, which are available, e.g., in ref 41, rather than calculated ab initio.

On the contrary, the effects of the Ln^{3+} ion and the interligand interactions on the ligand-localized excited levels in our approach are not neglected. The relative positions of these levels in the complex are determined taking into account the presence of Ln^{3+} ion explicitly by calculations of the entire complex.

The structure of the paper is as follows. In the next section, we describe some qualitative models of energy transfer in lanthanide complexes. We consider $T_1 \rightarrow {}^5D_j$ transfer, because it was shown in ref 28 that the $T_1 \rightarrow {}^5D_j$ transfer channel is several orders of magnitude more efficient than the direct $S_1 \rightarrow {}^5D_j$ channel. We include ligand relaxation in the triplet state into the scheme. Next, we describe the computational technique used to calculate the energy mismatch between T_1 and ^5D_j levels. Further, we verify our procedure on a series of Gd^{3+} complexes, for which experimental energies for ligand-localized triplet states are available. Finally, we apply the proposed approach to some typical phosphorescent emitters that differ in efficiency, namely, tris-thenoyltrifluoroacetate (tta) complexes of Eu^{3+} ($4f^6$) with bipyridine bipy and phenanthroline phen (Scheme 1). It is known (see refs 42 and 43 and references therein) that Eu(tta)$_3$phen is one of the most efficient Eu-based emitters, while bipyridine complexes are less efficient.

Models of Energy Transfer in OLEDs. Figure 1 illustrates a commonly accepted simple qualitative scheme ("antenna" model[44−46]) of excitation transfer in the emitting layer of OLEDs. An electron and a hole transferred to the emitting layer form an exciton. The excitons are trapped on host molecules, which constitute about 90% of the emitting layer (see refs 1, 2, and 4). The host molecules cannot directly transfer the excitation energy to Ln^{3+}, because they are spatially separated from Ln^{3+}. In addition, the energy gap between the T_1 energy of the host molecules and the excited-state levels of Ln^{3+} is usually large. The triplet excitation energy is transferred to a ligand in the lanthanide complex whose triplet-state energy is close enough to the T_1 energy of the host molecule. Next, the excitation energy is transferred to one of the excited levels of the lanthanide ion. The excited Ln^{3+} quickly relaxes to the lowest f−f excited state through internal conversion, from which emission occurs. Hence, the ligands in the complex serve as antennas receiving the triplet excitation from the host and transferring it to the Ln^{3+}.

dx.doi.org/10.1021/jp111303a |*J. Phys. Chem. A* 2011, 115, 4565–4573

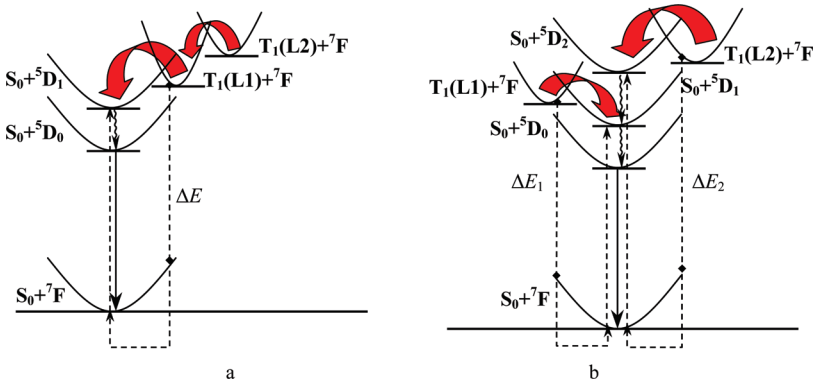

Figure 2. (a) Stepwise ligand-to-ligand-to-metal and (b) direct ligand-to-metal excitation transfer pathways. Solid arrows show radiative transitions. Wavy arrows denote internal conversion. Block arrows denote energy transfer. Dashed arrows show virtual nonradiative transitions in resonance energy transfer. Resonance condition means that for (a) $\Delta E \approx E(^7F \rightarrow {}^5D_1)$ and for (b) $\Delta E_1 \approx E(^7F \rightarrow {}^5D_1)$ and $\Delta E_2 \approx E(^7F \rightarrow {}^5D_2)$.

The relaxation of the excited-state structure occurs in $10^{-10}-10^{-14}$ s (which is comparable to the period of molecule vibrations), i.e., it is several orders of magnitude faster than energy-transfer processes ($10^{-6}-10^{-10}$ s).[12,47] Therefore, the structure relaxation cannot be ignored in the models. However, most energy-transfer schemes proposed before do not take into account the relaxation of the ligand structure in the excited state. Ligand relaxation in the triplet state was taken into account, for example, in refs 33−35.

If we take into account structure relaxation, each transfer event breaks into several steps: exciton capture, fast internal conversion to the lowest excited state (for a triplet exciton, it is T_1 state localized on a certain molecule), structure relaxation to the local minimum, and excitation transfer to the next molecule with an appropriate receiving triplet level. Figure 2 shows processes in the triplet-excited lanthanide complex after the ligand with the appropriate receiving triplet level captured the exciton from the host molecule. The ligand at which excitation is localized relaxes to the minimum of its lowest triplet state (Figure 2).

The adiabatic potential energy surfaces (PES) of the triplet states may have several minima corresponding to localization of the triplet excitation on different ligands. Figure 2 shows two possible ways of energy transfer from the ligands to the lanthanide ion: a stepwise transfer, in which excitation is transferred from ligand to ligand before it finally goes to the central ion (Figure 2a), and a direct energy transfer from a ligand to a sublevel of the emitting multiplet (^5D_j in Eu^{3+} and Tb^{3+}) (Figure 2b). Different ligands can transfer excitation to different sublevels of the emitting multiplet of Ln^{3+} (these sublevels are separated by only ~0.2−0.5 eV). Next, the excited Ln^{3+} ion can either emit light from one of these sublevels or, preferably, relax to the lowest sublevel and emit from it. Stepwise transfer is less efficient because each step may involve additional energy losses. The mechanism of energy transfer that occurs in a specific system depends on the relative positions of the local minima of the triplet states. Following ref 47, in Figure 2 we show virtual transitions in energy transfer by dashed lines and actual transitions by block arrows. Some authors (for example, ref 28) also propose a direct $S_1 \rightarrow {}^5D_j$ transfer channel. In addition, excitation back-transfer may complicate direct transfer processes.[6,7,13,16,23,25]

Resonance between donor and acceptor excitation energies is a necessary condition for energy transfer to be efficient.[47] Resonance condition means that, for the case shown in Figure 2a, $\Delta E \approx E(^7F \rightarrow {}^5D_1)$ and, for the case shown in Figure 2b, $\Delta E_1 \approx E(^7F \rightarrow {}^5D_1)$ and $\Delta E_2 \approx E(^7F \rightarrow {}^5D_2)$. Additionally, the absolute energy gap between the donor and the acceptor states should be small: $E(T_1(L) + {}^7F) \approx E(S_0(L) + {}^5D_j)$. On the other hand, the exact matching of these levels is not required, because (a) a small mismatch of the order of the mean thermal energy or even more can be insignificant from the practical point of view and (b) when the levels are nearly degenerate excitation back transfer, which can occur in this case, may decrease the overall efficiency of Ln^{3+} ion pumping.

Charge-transfer processes (ligand-to-ligand LLCT, metal-to-ligand MLCT, or ligand-to-metal LMCT), which result in the spatial separation of the electron−hole pair,[14,24,26,48] may interfere with efficient energy transfer when the corresponding states fall in the same energy range as the ligand-localized triplet states. However, it is known[6,7] that the complexes considered in this work do not have low-lying LMCT states. In addition, ^5D_j states can be quenched by vibrational energy transfer.[47,49] At present, we do not include into consideration LMCT and vibrational quenching effects.

Multipolar and exchange mechanisms of nonradiative energy transfer from the ligands to the central ion in lanthanide compounds are usually distinguished to describe elementary events in the overall transfer process.[12,50,51] The selection rules for these mechanisms are different and in many cases complementary. For example, the multipolar mechanism facilitates energy transfer from the excited triplet on a ligand to the $^5D_2$ level of Eu^{3+}, while the exchange mechanism facilitates transfer to $^5D_1$. Therefore, the selection rules are less important for determining the possibility of energy transfer than the energy mismatch.

As mentioned above, commonly accepted antenna models of energy transfer in Ln^{3+} complexes are based on the assumption that the excitation in the complexes is ligand localized. This assumption is supported by a number of theoretical considerations[34,35] and experimental observations.[26,46,52] Thus, in different lanthanide complexes containing the same organic ligand, the positions of the excitation and emission bands associated with this ligand only slightly differ from each other (see, for example, refs 26, 46, and 52). This indicates that these excited states are only slightly affected by the nature of the central ion and other ligands and excitation is localized on the corresponding ligand. Theoretical results of refs 34 and 35 also show that excitation is localized on one of the ligands.

On the basis of the above considerations, we use the following scheme to analyze the efficiency of energy transfer. The excitation energy is transferred to the lanthanide ion from the relaxed T_1 excited state of the complex. Because in heteroleptic complexes the

T_1 excited state can be localized on different ligands, we considered various possibilities for localization by means of finding various local minima on the T_1 potential energy surface of the entire complex. If the energy of the vertical $T_1 \rightarrow S_0$ transition from a local minimum (ΔE) is close to some $^7F_0 \rightarrow {}^5D_j$ transition energy of the free Ln^{3+} ion, the excitation energy can be transferred to this level (resonance condition is fulfilled). The energy mismatch may be of the order of the thermal energy. If $\Delta E(T_1 \rightarrow S_0)$ is slightly lower than $\Delta E(^5D_j \rightarrow {}^7F_0)$, the deficient energy can, nevertheless, be supplied through the thermal excitation of the ligand. Such a situation, however, results in the temperature dependence of the transfer efficiency in such systems[6] and high back-transfer rate. If $\Delta E(T_1 \rightarrow S_0)$ is slightly higher than $\Delta E(^5D_j \rightarrow {}^7F_0)$, the excess energy is dissipated in the material.

COMPUTATIONAL TECHNIQUE

Before presenting in detail our computational technique, we give some preliminary comments.

Our test calculations of heteroleptic complexes by the U-DFT and RO-DFT methods with the PBE and PBE0 functionals showed that the lowest triplet excitations in the ground-state geometry are delocalized over ligands. The subsequent optimization of the triplet excited-state geometry led to the localization of triplet excitations on only one ligand, which was assisted by the corresponding structural changes in the ligand bearing the excitation. When we started the procedure of optimization with a structure in which the geometry of a certain ligand was properly predistorted, we managed to obtain the triplet state localized on each tta fragment but failed to obtain the triplet state localized on phen. This means that, within DFT, the T_1 PES has three minima corresponding to excitation localized on the three tta fragments and no minimum with excitation is localized on phen.

On the other hand, as shown in ref 34, complete active space self-consistent field (CASSCF) calculations predict localized quasi-degenerate triplet states even in the ground-state geometry, that is, both singly occupied natural orbitals are localized on the same one ligand. The geometry of each of these states can further be optimized independently to obtain a properly localized minimum.

On the basis of the above considerations and having in mind that ligand-localized excited states might be quasi-degenerate in energy at the ground-state structure, we used multireference electronic structure methods in our calculations. Our approach was based on the CASSCF reference wave function corrected for dynamic correlation effects at the second-order multireference perturbation theory. Such an approach was found sufficiently accurate when applied to various organic chromophores[53,54] and inorganic phosphors.[55] Recently, an extended multiconfiguration quasi-degenerate perturbation theory (XMCQDPT)[56−58] was developed to improve the conventional multiconfiguration quasi-degenerate perturbation theory (MCQDPT).[59] It was found that XMCQDPT2 is more robust than the original MCQDPT2 method,[56,57,60] especially near conical intersections and avoided crossings.

CASSCF and XMCQDPT2 calculations were performed using the Firefly (formerly known as PC-GAMESS) program package.[61] In these calculations, the 6-31G(d,p) basis set was used on all atoms except lanthanide(III) ions, for which the scalar relativistic 4f-in-core pseudopotentials (ECP52MWB for Eu^{3+} and ECP53MWB for Gd^{3+}) with the associated valence basis sets were used.[36,37] Indeed, only scalar relativistic effects associated with the heavy Ln atom must be taken into account, while a standard nonrelativistic approximation is relevant for the ligands consisting of only light atoms.

The geometries of the complexes in the ground and triplet states were fully optimized by the state-specific CASSCF (SS-CASSCF/6-31G(d,p)) method. Next, the vertical excitation energies were calculated at the optimized ground-state and triplet-state geometries using the state-averaged CASSCF (SA-CASSCF) method, and the calculated positions of the ligand-localized triplet and singlet levels were corrected by the XMCQDPT2 method. Separate calculations were performed for singlets and triplets in all cases. We denote this technique as XMCQDPT2/SA-CASSCF.

The active space in CASSCF calculations should include the necessary amount of occupied and unoccupied ligand orbitals separated by an energy gap from other orbitals. In the heteroleptic complexes, the active space included one HOMO and one LUMO from each tta and one HOMO and two LUMOs from bipy (CASSCF(8,9)) or two HOMOs and two LUMOs from phen (CASSCF(10,10)). In the model complexes, we expanded the active space so as to include as many π orbitals of the organic ligand as possible (up to CASSCF(10,10) in $Gd(phen)Cl_2(H_2O)_4$ and CASSCF(12,12) in $Gd(bipy)Cl(H_2O)_5$).

In the SA-CASSCF calculations, the following states were averaged: for bipy, we took four singly excited singlet states plus S_0 or four singly excited triplet states; for phen, there were five singly excited singlet states plus S_0 or five singly excited triplet states. The effective Hamiltonian H_{eff} in XMCQDPT2 calculations should include a sufficient amount of extra states to ensure the convergence of perturbation estimates, as recommended in ref 58. Our present XMCQDPT2 calculations for heteroleptic complexes accounted for the 34 lowest states (including the S_0 state) in the case of singlets and the 34 lowest states in the case of triplets. For model complexes, the 20 lowest states of each multiplicity were taken into account.

The energies of the ligand-localized triplet levels were compared with the positions of the receiving and emitting levels of the Ln^{3+} ions taken from the experimental database.[41] In this model, high-level ab initio calculations of the entire complexes can be performed for almost any sort of ligands.

RESULTS AND DISCUSSION

Validation of Predictions of Ligand-Localized Triplet States in Lanthanide Complexes and Comparison with Experimental Data. The calculated ligand-localized triplet levels in heteroleptic lanthanide complexes are usually compared with the experimental data available for Gd^{3+} ($4f^7$), La^{3+} ($4f^0$), or Lu^{3+} ($4f^{14}$) complexes (see, for example, refs 34 and 35). In such complexes, the phosphorescence of the ligand of interest in the presence of Ln^{3+} can be observed without being masked by the emission from the lanthanide or other ligands.

We used experimental data of refs 26 and 62−65 for tta, phen, and bipy in Gd^{3+} complexes. References 62 and 63 give the position of the triplet level of tta obtained from the phosphorescence of $Gd(tta)_3$, and ref 64 gives the position of the triplet level of phen obtained from the phosphorescence of $Gd(phen)_2Cl_3(H_2O)_2$. Reference 65 gives the position of the triplet level of bipy in $Gd(bipy)_2Cl_3(H_2O)_2$. Reference 26 gives the triplet energies of phen and bipy in heteroleptic complexes of Gd^{3+} with various dithiocarbamates and phen or bipy, respectively. Slightly different triplet energies of phen in the complexes with different dithiocarbamates can be attributed to the interligand interactions. All experimental transition energies have been determined for the 0−0 transitions.

Table 1. S_0-T_1 transition Energies (eV) of the Organic Ligands in the Model Complexes

complex	active space	$\Delta E(S_0 \rightarrow T_1)$	$\Delta E(T_1 \rightarrow S_0)$	ΔE_{relax}	ΔE_{adiab}	ΔE_{0-0} exp
$Gd(tta)_3$	(6,6)	3.35	1.88	1.47	2.36	2.535[a]
$Gd(phen)(H_2O)_4Cl_2^+$	(10,10)	3.30	2.31	0.99	2.88	2.68[b], 2.725[b]
$Gd(phen)_2(H_2O)_3Cl^{2+}$	(8,8)	3.93	2.77	1.16	3.61	
$Gd(phen)_2(H_2O)_2Cl_2^+$	(8,8)	3.94	2.50	1.44	3.03	2.737[c]
$Gd(bipy)(H_2O)_5Cl^{2+}$	(12,12)	3.53	2.28	1.25	2.78	2.725[d], 2.87[b]

[a] References 62 and 63. [b] Reference 26 data for $Gd(R_2NCS_2)_3(bipy)$ and $Gd(R_2NCS_2)_3(phen)$. [c] Reference 64. [d] Reference 65.

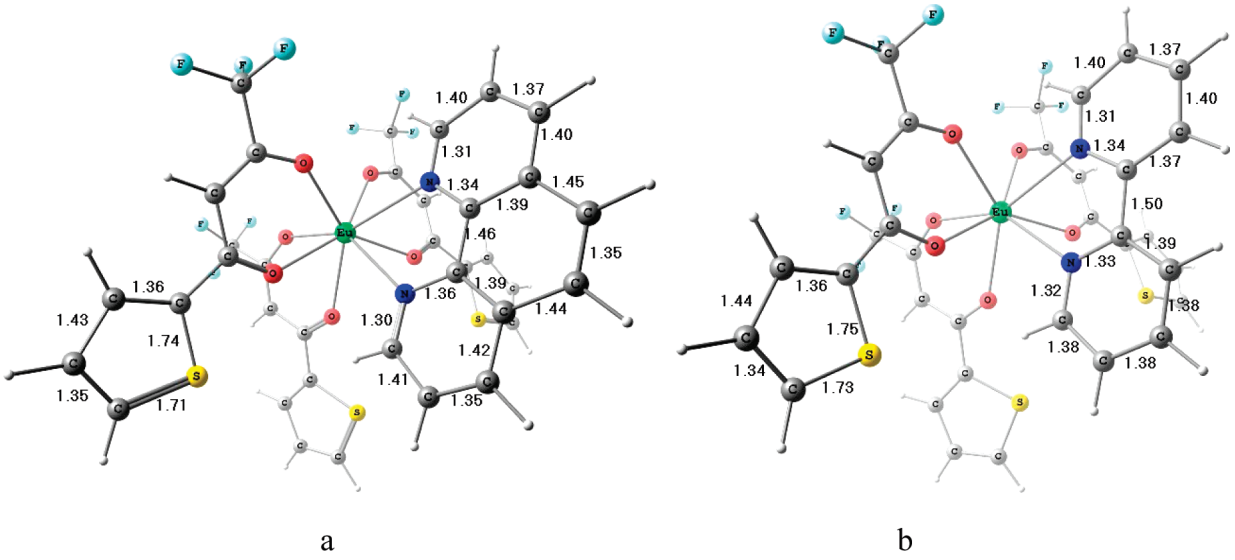

Figure 3. Optimized ground-state structures of (a) $Eu(tta)_3phen$ and (b) $Eu(tta)_3bipy$ (bond lengths in Angstroms).

We calculated the positions of the T_1 levels localized on the tta, phen, and bipy ligands in a series of model complexes $Gd(phen)_xCl_y(H_2O)_z$, $Gd(bipy)_xCl_y(H_2O)_z$ (x = 1, 2, y = 1, 2, z = 2−5), and $Gd(tta)_3$ and compared them with the available experimental data. All the T_1 states turned out to be localized on a certain organic ligand. The starting geometries for optimization were taken from the X-ray diffraction data of refs 33, 66, and 67 The results are shown in Table 1. $\Delta E(S_0 \rightarrow T_1)$ is the vertical transition energy calculated at the optimized ground-state geometry. $\Delta E(T_1 \rightarrow S_0)$ is the vertical transition energy calculated at the optimized triplet-state geometry. ΔE_{relax} is the difference between the vertical $S_0 \rightarrow T_1$ and $T_1 \rightarrow S_0$ transition energies; this increment in the case of forbidden transitions is an analog of the Stokes shift for allowed transitions. ΔE_{adiab} is the difference between the energy minima of the T_1 and S_0 states.

Expanding the active space from (8,8) to (12,12) for $Gd(bipy)(H_2O)_5Cl^{2+}$ had only a slight (~0.01 eV) effect on the final XMCQDPT2 value of the transition energy.

We compare the calculated adiabatic transitions with the experimental 0−0 transition values. The energies of 0−0 transitions can be calculated if zero-point energy (ZPE) corrections are taken into account for both T_1 and S_0. According to ref 34 the difference of ZPE in T_1 and S_0 can be more than 0.1 eV. However, we did not include the ZPE corrections, because of their high computational cost. The agreement between the calculated ΔE_{adiab} and the experimental ΔE_{0-0} is rather good, having in mind that no ZPE corrections were made.

In the relaxed triplet state, the ligand on which the excitation is localized changes its geometry most significantly while the other ligands virtually retain their ground-state geometries. When a complex contains several ligands of the same type, this results in a noticeable symmetry breaking.

For the tta ligand, the relaxation energy is 1.47 eV. The geometry of the excited ligand changes only in the thienyl ring: the C−C bond opposite to the S atom becomes shorter by more than 0.1 A, the adjacent C−C bonds become longer by approximately the same value, both C−S bonds become longer, and the C−H bond near the S atom comes out of the plane by ~22°. Similar effects (localization of the triplet state on one of the ligands and out-of-plane distortion of the excited ligand) were observed in ref 34.

For phen and bipy ligands, the reorganization energy is in the range of ~1−1.5 eV, depending on the complex composition. Phen exhibits only changes in the bond lengths and remains planar. On the contrary, bipy becomes nonplanar because of out-of-plane distortions of both pyridine rings (no twisting around central C−C bond is observed). Hence, the structure relaxation in the triplet state cannot be neglected in the calculations.

Simulation of the Level Positions in the Heteroleptic Complexes. Eu^{3+} tris-diketonate complexes are known as very good emitters when proper diketonate is used.[43] Thenoyltrifluoroacetate, tta, is one of these good antenna ligands, but the coordination sphere of Eu^{3+} requires more ligands. In $Eu(tta)_3$ water frequently fills the coordination sphere. As a result, $Eu(tta)_3(H_2O)_2$ is only weakly luminescent because water quenches Eu^{3+} emission. The solution is to replace water by some organic ligands. When energy-transferring antenna ligands

dx.doi.org/10.1021/jp111303a |J. Phys. Chem. A 2011, 115, 4565–4573

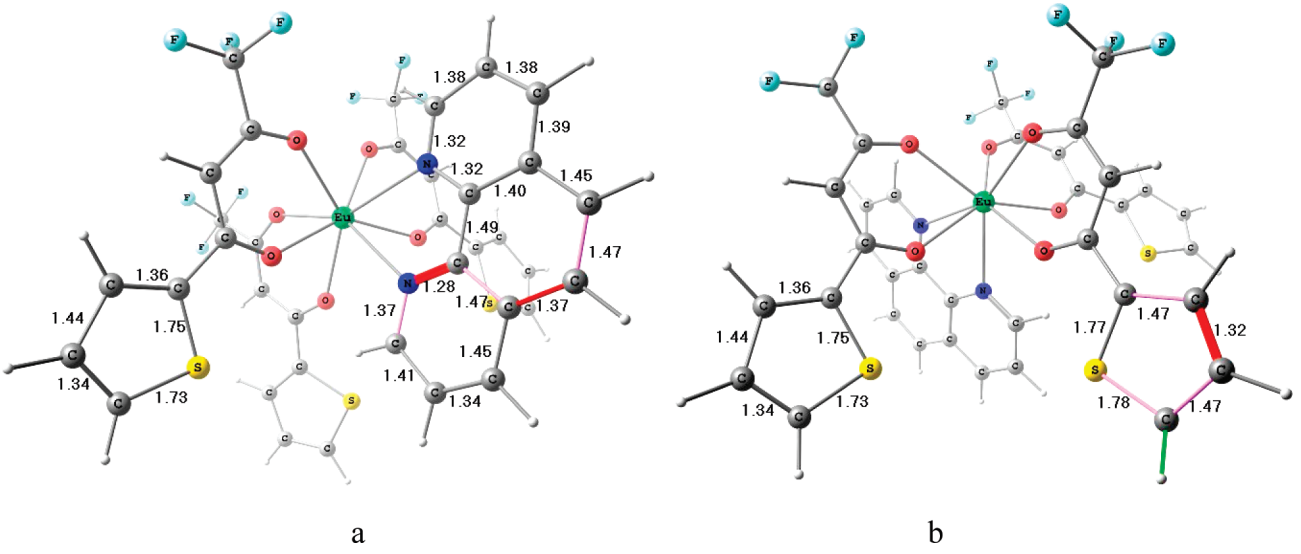

Figure 4. Optimized triplet-state structures of $Eu(tta)_3phen$ with triplet localization (a) on phen ($Eu(tta)_3phen^*$) and (b) on tta ($Eu(tta)_2tta^*phen$). Pink lines show a noticeable bond lengthening relative to the ground-state structure, red lines show bond shortening, and green lines show bonds that come out of plane.

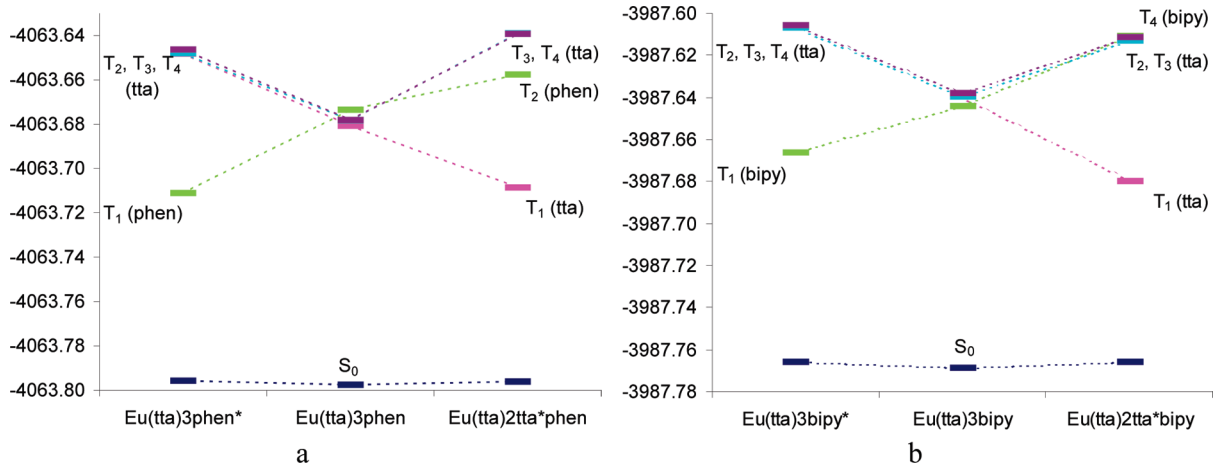

Figure 5. Positions of the triplet levels in (a) $Eu(tta)_3phen$ and (b) $Eu(tta)_3bipy$ in the ground-state and relaxed-triplet geometries ("$Eu(tta)_3phen$" or "$Eu(tta)_3bipy$", "$Eu(tta)_2tta^*phen$" or "$Eu(tta)_2tta^*bipy$", and "$Eu(tta)_3phen^*$" or "$Eu(tta)_3bipy^*$" on the category axis denote corresponding relaxed geometries, while the labels on the data points denote excitation localization in the corresponding triplet state; the energies are in au).

L are used, the emission intensity increases many times. Such Lewis bases as phen and bipy are good candidates for this role. It is known that the emission intensity of $Eu(tta)_3bipy$ is lower than that of $Eu(tta)_3phen$, because of which the latter is more popular as an emitter in OLEDs.[43]

Here, we will use the results of our calculations to explain the difference in the efficiency of two heterocyclic antenna ligands, phen and bipy.

The geometries of the ground states of $Eu(tta)_3phen$ and $Eu(tta)_3bipy$ were fully optimized at the SS-CASSCF/6-31G(d,p) level. The starting structures for geometry optimizations were taken from refs 68 and 69. The optimized structures are shown in Figure 3.

We calculated the triplet energies of the heteroleptic β-diketonate complexes in their ground-state geometry. In $Eu(tta)_3phen$, the three lowest triplets are localized on diketonate ligands while the fourth triplet is localized on phen. In $Eu(tta)_3bipy$, the first triplet is localized on bipy while the next three triplets are localized on tta ligands. The energy gaps between the ligand-localized triplet levels are rather small (~0.1 eV) in both complexes (see Figure 5), which allows us to treat these levels as quasi-degenerate.

Ligand Relaxation in the Triplet State. We optimized the geometries for each of the four lowest triplet states in $Eu(tta)_3phen$ and $Eu(tta)_3bipy$. The relaxed triplet structures of $Eu(tta)_3phen$ and $Eu(tta)_3bipy$ are shown in Figures 4 and 7, respectively. We denote the excited molecules as $Eu(tta)_3phen^*$ or $Eu(tta)_3bipy^*$ when the excitation is localized on phen or bipy, respectively, and $Eu(tta)_2tta^*phen$ or $Eu(tta)_2tta^*bipy$ when the excitation is localized on tta. The structural changes in the ligand-localized triplet states are very similar to those observed in the model Gd^{3+} complexes. When the triplet excitation is localized on tta, three quasi-degenerate minima correspond to similar structural changes in each tta

dx.doi.org/10.1021/jp111303a |J. Phys. Chem. A 2011, 115, 4565–4573

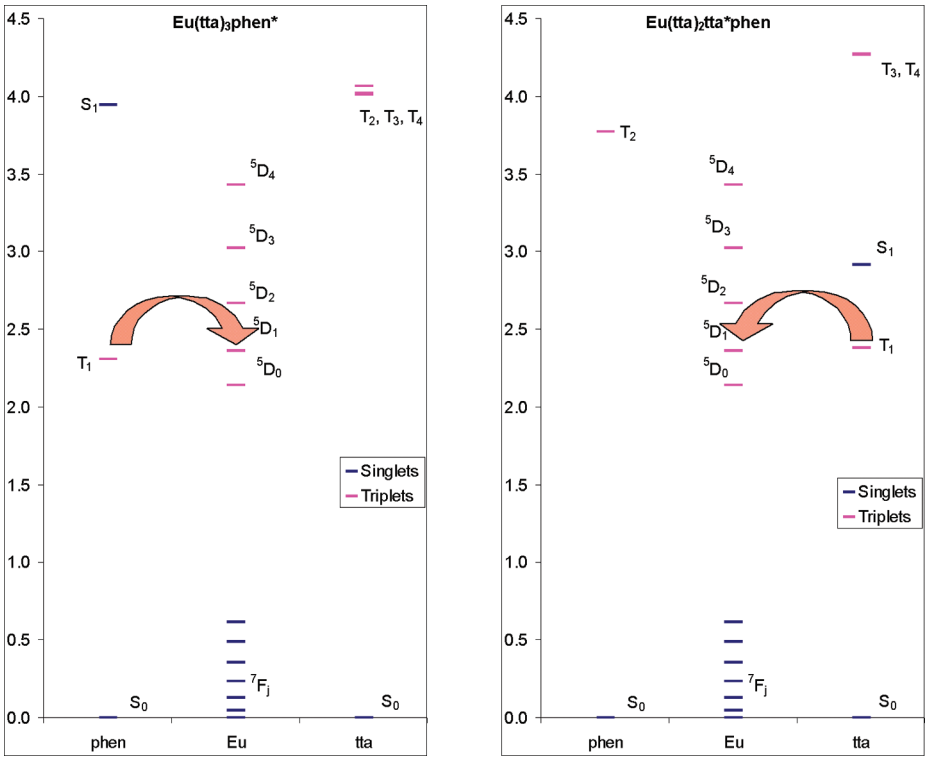

Figure 6. Calculated lowest triplet levels (eV) of $Eu(tta)_3phen$ relative to the experimental quintet levels of Eu^{3+} for the relaxed geometries of different intraligand triplet states. Block arrows show energy-transfer pathways.

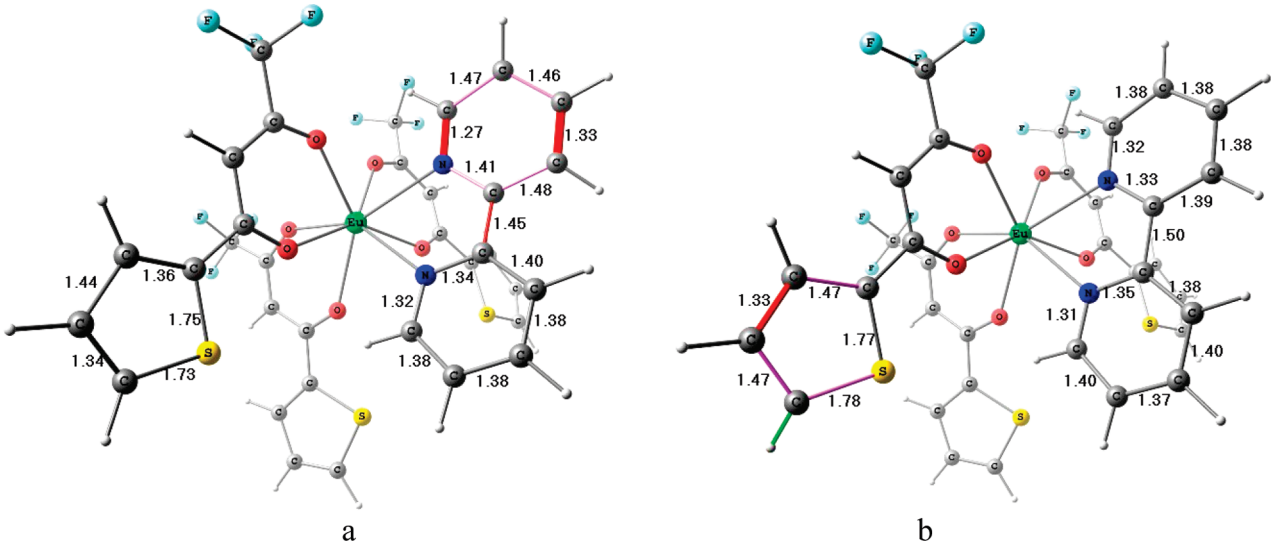

Figure 7. Optimized triplet-state structures of $Eu(tta)_3bipy$ with triplet localization on (a) bipy ($Eu(tta)_3bipy^*$) and (b) tta ($Eu(tta)_2tta^*bipy$). Pink lines indicate a noticeable bond lengthening relative to the ground-state structure, red lines correspond to a bond shortening, and green lines show bonds that come out of the plane.

fragment. Hence, we show the results for only one tta-localized triplet state.

For all the obtained triplet structures of $Eu(tta)_3phen$ and $Eu(tta)_3bipy$, we calculated the energies of the lowest triplet and singlet levels (Tables S1 and S2 in Supporting Information). The potential energy surface in the ground state seems to be rather flat: the ground-state energies in the relaxed-triplet geometries are ~1 kcal/mol higher than the energy in the ground-state geometry.

The energies of the relaxed structures with triplets localized on any of the tta fragments (opposite to phen, on the left, or on the right of phen) and on phen are quasi-degenerate, i.e., the corresponding minima are of an almost equal depth. At the optimized $Eu(tta)_2tta^*phen$ and $Eu(tta)_3phen^*$ geometries, the triplet state localized on the respective distorted ligand is lowered in energy (because these geometries correspond to the energy minima of the corresponding terms) while the vertical energies of

dx.doi.org/10.1021/jp111303a |J. Phys. Chem. A 2011, 115, 4565–4573

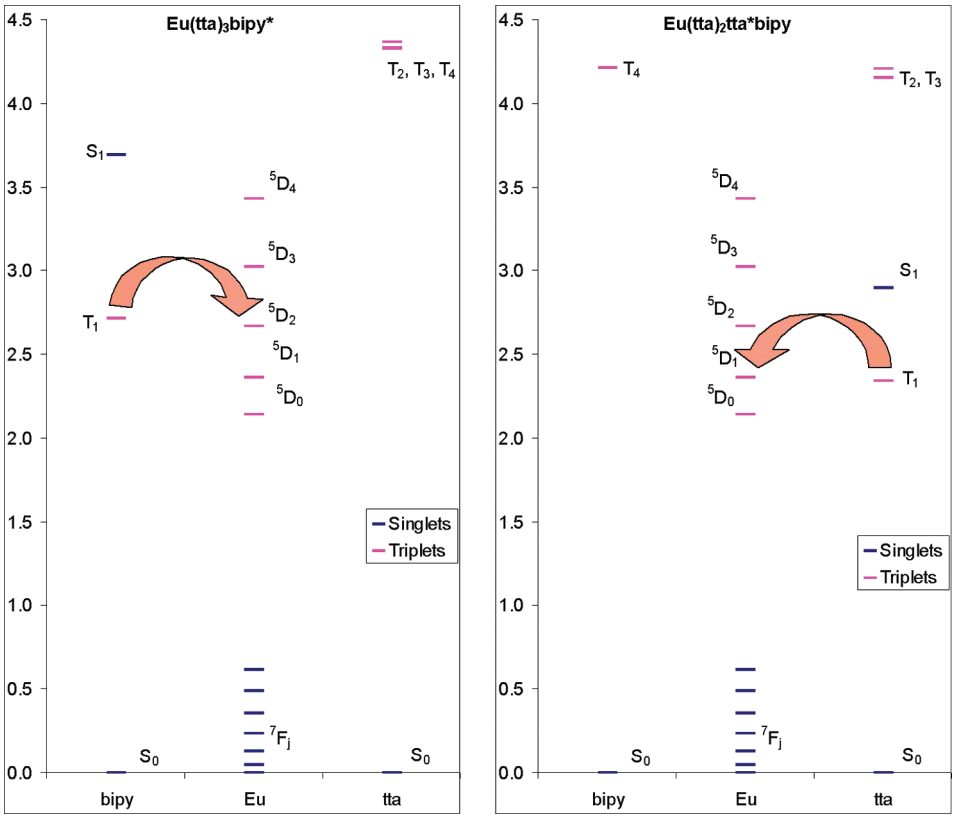

Figure 8. Calculated lowest triplet levels (eV) of $Eu(tta)_3bipy$ relative to the experimental quintet levels of Eu^{3+} for the relaxed geometries of different intraligand triplet states. Block arrows show energy-transfer pathways.

the triplets localized on the other (undistorted) ligands noticeably increase as compared to their values at the S_0 geometry (Figure 5a). Both tta- and phen-localized triplets are almost degenerate with the $^5D_1$ level of Eu^{3+}, which facilitates efficient energy transfer to this level from one of the lowest vibrational sublevels in these minima (Figure 6).

A similar picture is observed for $Eu(tta)_3bipy$. The structural changes in the tta fragments are the same as in $Eu(tta)_3phen$, while the changes in the bipy fragment resemble those in $Gd(bipy)(H_2O)_5Cl^{2+}$ (Figure 7). The energies of $Eu(tta)_2tta^*bipy$ minima are almost the same as in $Eu(tta)_2tta^*phen$, while the energy of $Eu(tta)_3bipy^*$ minimum is higher (Figure 5b) and is quasi-degenerate with the $^5D_2$ level of Eu^{3+}. This means that the tta-localized triplets can transfer energy to the $^5D_1$ level of Eu^{3+}, while the bipy-localized triplet can transfer energy only to the $^5D_2$ level (Figure 8).

Such an arrangement of the ligand-localized triplet states indicates that the excitation energy in $Eu(tta)_3phen$ is transferred from both different ligands to the same acceptor level of Eu^{3+}, while in $Eu(tta)_3bipy$ additional steps (either ligand-to-ligand energy transfer or intralanthanide conversion between *j* multiplets of the ^5D states) are required. These additional steps must reduce the efficiency of bipy as antenna, which is in agreement with the experimental observations (see refs 42 and 43 and references therein).

CONCLUSIONS

In order to describe energy transfer in phosphorescent emitters made of lanthanide complexes with organic ligands, an ab initio procedure was developed for calculation of the lowest singlet and triplet levels in the complexes. These states turn out to be localized on one of the ligands. The procedure is based on the XMCQDPT2/CASSCF approach and on the 4f-in-core pseudopotential approximation (the latter reduces the computational cost substantially). The importance of taking into account the structure relaxation in the triplet excited state of the complex is demonstrated. The procedure essentially involves geometry optimization of the lowest triplet states, which results in localization of excitation on a certain ligand. Our case-study calculations of the lowest triplet levels in the relaxed triplet structures in $Eu(tta)_3phen$ and $Eu(tta)_3bipy$ provide a possible explanation for why energy transfer in the former complex is more efficient than in the latter one. We believe that the developed procedure might be helpful for predicting efficient antenna ligands for organic light-emitting devices.

ASSOCIATED CONTENT

Supporting Information. Calculated energies of the ligand-localized triplet levels in $Eu(tta)_3phen$ and $Eu(tta)_3bipy$ for the relaxed triplet geometries. This material is available free of charge via the Internet at http://pubs.acs.org.

AUTHOR INFORMATION

Corresponding Author
*E-mail: sanya@photonics.ru.

ACKNOWLEDGMENT

This work was supported by the Russian Foundation for Basic Research (project no. 09-03-00993-a), the Presidium of the

Russian Academy of Sciences, and the Ministry of Education and Science of the Russian Federation (contract no. 02.523.11.3014). The calculations were performed using the facilities of the Joint Supercomputer Center, Russian Academy of Sciences. We thank Dr. A. A. Granovsky (Firefly project) for helpful discussions.

REFERENCES

(1) Kalinowski, J. *Organic Light-Emitting Diodes: Principles, Characteristics, and Processes*; Marcel Dekker: New York, 2005.
(2) Müllen, K.; Scherf, U. *Organic Light Emitting Devices. Synthesis, Properties and Applications*; Wiley-VCH: Weinhein, 2006.
(3) The Promise of Solid State Lighting for General Illumination. *Light Emitting Diodes (LEDs) and Organic Light Emitting Diodes (OLEDs) for General Illumination Update 2002. An OIDA Technology Roadmap*; Stolka M., Ed.; OIDA: Washington, DC, 2002.
(4) Yersin, H. *Highly Efficient OLEDs with Phosphorescent Materials*; Wiley-VCH: Weinheim, 2008.
(5) Ronda, C. *Luminescence: From Theory to Applications*; Wiley-VCH: Weinheim, 2008.
(6) Eliseeva, S.; Bünzli, J.-C. G. *Chem. Soc. Rev.* **2010**, *39*, 189.
(7) Bünzli, J.-C. G.; Chauvin, A.-S.; Kim, H. K.; Deiters, E.; Eliseeva, S. V. *Coord. Chem. Rev.* **2010**, *254*, 2623.
(8) Sato, S.; Wada, M. *Bull. Chem. Soc. Jpn.* **1970**, *43*, 1955.
(9) Latva, M.; Takalo, H.; Mukkala, V.-M.; Matachescu, C.; Rodríguez-Ubis, J. C.; Kankare, J. *J. Lumin.* **1997**, *75*, 149.
(10) de Andrade, A. V. M.; da Costa, N. B., Jr.; Simas, A. M.; de Sá, G. F. *Chem. Phys. Lett.* **1994**, *227*, 349.
(11) de Andrade, A. V. M.; da Costa, N. B., Jr.; Simas, A. M.; de Sá, G. F. *J. Alloys Compd.* **1995**, *225*, 55.
(12) de Andrade, A. V. M.; Longo, R. L.; Simas, A. M.; de Sá, G. F. *J. Chem. Soc., Faraday Trans.* **1996**, *92*, 1835.
(13) de Andrade, A. V. M.; da Costa, N. B., Jr.; Longo, R. L.; Malta, O. L.; Simas, A. M.; de Sá, G. F. *Mol. Eng.* **1997**, *7*, 293.
(14) Malta, O. L.; Brito, H. F.; Menezes, J. F. S.; Gonçalves e Silva, F. R.; Alves, S., Jr.; Farias, F. S., Jr.; de Andrade, A. V. M. *J. Lumin.* **1997**, *75*, 255.
(15) Malta, O. L.; Brito, H. F.; Menezes, J. F. S.; Gonçalves e Silva, F. R.; de Mello Donegá, C.; Alves, S., Jr. *Chem. Phys. Lett.* **1998**, *282*, 233.
(16) de Sá, G. F.; Malta, O. L.; de Mello Donegá, C.; Simas, A. M.; Longo, R. L.; Santa-Cruz, P. A.; da Silva, E. F. *Coord. Chem. Rev.* **2000**, *196*, 165.
(17) Faustino, W. M.; Rocha, G. B.; Gonçalves e Silva, F. R.; Malta, O. L.; de Sá, G. F.; Simas, A. M. *J. Mol. Struct. (THEOCHEM)* **2000**, *527*, 245.
(18) Longo, R.; Gonçalves e Silva, F. R.; Malta, O. L. *Chem. Phys. Lett.* **2000**, *328*, 67.
(19) Albuquerque, R. Q.; Rocha, G. B.; Malta, O. L.; Porcher, P. *Chem. Phys. Lett.* **2000**, *331*, 519.
(20) Batista, H. J.; Longo, R. L. *Int. J. Quantum Chem.* **2002**, *90*, 924.
(21) Rocha, G. B.; Freire, R. O.; da Costa, N. B., Jr.; de Sá, G. F.; Simas, A. M. *Inorg. Chem.* **2004**, *43*, 2346.
(22) Freire, R. O.; Rocha, G. B.; Simas, A. M. *Inorg. Chem.* **2005**, *44*, 3299.
(23) Faustino, W. M.; Malta, O. L.; de Sá, G. F. *J. Chem. Phys.* **2005**, *122*, 054109.
(24) Faustino, W. M.; Junior, S. A.; Thompson, L. C.; de Sá, G. F.; Malta, O. L.; Simas, A. M. *Int. J. Quantum Chem.* **2005**, *103*, 572.
(25) Faustino, W. M.; Malta, O. L.; de Sá, G. F. *Chem. Phys. Lett.* **2006**, *429*, 595.
(26) Faustino, W. M.; Malta, O. L.; Teotonio, E. E. S.; Brito, H. F.; Simas, A. M.; de Sá, G. F. *J. Phys. Chem. A* **2006**, *110*, 2510.
(27) Freire, R. O.; Simas, A. M. *J. Chem. Theory Comput.* **2010**, *6*, 2019.
(28) dos Santos, E. R.; Freire, R. O.; da Costa, N. B., Jr.; Almeida Paz, F. A.; de Simone, C. A.; Junior, S. A.; Araujo, A. A. S.; Nunes, L. A. O.; de Mesquita, M. E.; Rodrigues, M. O. *J. Phys. Chem. A* **2010**, *114*, 7928.
(29) Gutierrez, F.; Rabbe, C.; Poteau, R.; Daudey, J. P. *J. Phys. Chem. A* **2005**, *109*, 4325.
(30) Aiga, F.; Iwanaga, H.; Amano, A. *J. Phys. Chem. A* **2005**, *109*, 11312.
(31) Guillaumont, D.; Bazin, H.; Benech, J. M.; Boyer, M.; Mathis, G. *ChemPhysChem* **2007**, *8*, 480.
(32) Li, X. N.; Wu, Z. J.; Si, Z. J.; Zhou, L.; Liu, X. J.; Zhang, H. J. *Phys. Chem. Chem. Phys.* **2009**, *11*, 9687.
(33) Puntus, L. N.; Lyssenko, K. A.; Pekareva, I. S.; Bünzli, J.-C.G. *J. Phys. Chem. B* **2009**, *113*, 9265.
(34) Gutierrez, F.; Tedeschi, C.; Maron, L.; Daudey, J.-P.; Poteau, R.; Azema, J.; Tisnès, P.; Picard, C. *Dalton Trans.* **2004**, 1334.
(35) Gutierrez, F.; Tedeschi, C.; Maron, L.; Daudey, J.-P.; Azema, J.; Tisnès, P.; Picard, C.; Poteau, R. *J. Mol. Struct. (THEOCHEM)* **2005**, *756*, 151.
(36) Dolg, M.; Stoll, H.; Savin, A.; Preuss, H. *Theor. Chim. Acta* **1989**, *75*, 173.
(37) Dolg, M.; Stoll, H.; Preuss, H. *Theor. Chim. Acta* **1993**, *85*, 441.
(38) Casida, M. E. *J. Mol. Struct. (THEOCHEM)* **2009**, *914*, 3.
(39) Cramer, C. J.; Truhlar, D. G. *Phys. Chem. Chem. Phys.* **2009**, *11*, 10757.
(40) Dreuw, A.; Head-Gordon, M. *Chem. Rev.* **2005**, *105*, 4009.
(41) Ralchenko, Yu.; Kramida, A. E.; Reader, J.; NIST ASD Team (2008). *NIST Atomic Spectra Database*, version 3.1.5; Available at http://physics.nist.gov/asd3 [July 15, 2010]. National Institute of Standards and Technology: Gaithersburg, MD, 2010.
(42) Katkova, M. A.; Vitukhnovsky, A. G.; Bochkarev, M. N. *Russ. Chem. Rev.* **2005**, *74*, 1089.
(43) Binnemans, K. *Chem. Rev.* **2009**, *109*, 4283.
(44) Whan, R. E.; Crosby, G. A. *J. Mol. Spectrosc.* **1962**, *8*, 315.
(45) Crosby, G. A.; Whan, R. E.; Alire, R. M. *J. Chem. Phys.* **1961**, *34*, 743.
(46) Crosby, G. A.; Whan, R. E.; Freeman, J. J. *J. Phys. Chem.* **1962**, *66*, 2493.
(47) Ermolaev, V. L.; Sveshnikova, E. B.; Bodunov, E. N. *Physics-Uspekhi* **1996**, *39* (3), 261.
(48) Fonger, W. H.; Struck, C. W. *J. Chem. Phys.* **1970**, *52*, 6364.
(49) Campos, A. F.; Meijerink, A.; de Mello Donegá, C.; Malta, O. L. *J. Phys. Chem. Solids* **2000**, *61*, 1489.
(50) Malta, O. L. *J. Lumin.* **1997**, *71*, 229.
(51) Malta, O. L. *J. Non-Cryst. Solids* **2008**, *354*, 4770.
(52) Tobita, S.; Arakawa, M.; Tanaka, I. *J. Phys. Chem.* **1985**, *89*, 5649.
(53) Bravaya, K. B.; Bochenkova, A. V.; Granovsky, A. A.; Savitsky, A. P.; Nemukhin, A. V. *J. Phys. Chem. A* **2008**, *112*, 8804.
(54) Bravaya, K.; Bochenkova, A.; Granovsky, A.; Nemukhin, A. *J. Am. Chem. Soc.* **2007**, *129*, 13035.
(55) Krasikov, D. N.; Scherbinin, A. V.; Vasil'ev, A. N.; Kamenskikh, I. A.; Mikhailin, V. V. *J. Lumin.* **2008**, *128*, 1748.
(56) XMCQDPT (Extended Multi-Configuration Quasi-Degenerate Perturbation Theory) is an improved version of the MCQDPT[59] approach recently developed by Dr. Alex A. Granovsky of MSU and is currently specific to PC GAMESS/Firefly. http://classic.chem.msu.su/gran/gamess/xmcqdpt.pdf.
(57) http://classic.chem.msu.su/gran/gamess/conic-qdpt.pdf
(58) Granovsky, A. A. *J. Chem. Phys.*, submitted for publication.
(59) Nakano, H. *J. Chem. Phys.* **1993**, *99*, 7983.
(60) http://classic.chem.msu.su/gran/gamess/mcqdpt-vs-xmcqdpt-in-O3.pdf.
(61) http://classic.chem.msu.su/gran/gamess/.
(62) Brinen, J. S.; Halverson, F.; Leto, J. R. *J. Chem. Phys.* **1965**, *42*, 4213.
(63) Dawson, W. R.; Kropp, J. L.; Windsor, M. W. *J. Chem. Phys.* **1966**, *45*, 2410.
(64) Bing, Y.; Hongjie, Z.; Shubin, W.; Jianzuan, N. *Spectrosc. Lett.* **1998**, *31* (3), 603.
(65) Puntus, L. N. *Helv. Chim. Acta* **2009**, *92*, 2552.
(66) Puntus, L. N.; Lyssenko, K. A.; Antipin, M. Yu.; Bünzli, J.-C. G. *Inorg. Chem.* **2008**, *47*, 11095.
(67) White, J. G. *Inorg. Chim. Acta* **1976**, *16*, 159.
(68) Xiao-Feng, Ch.; Xu-Hui, Z.; Yao-Hua, X.; Raj, S. S. S.; Ozturk, S.; Hoong-Kun, F.; Jing, M.; Xiao-Zeng, Y. *J. Mater. Chem.* **1999**, *9*, 2919.
(69) Hu, M.-L.; Huang, Z.-Y.; Cheng, Y.-Q.; Wang, S.; Lin, J.-J.; Hu, Y.; Xu, D.-J.; Xu, Y.-Z. *Chin. J. Chem.* **1999**, *17*, 637.